Gramillin A and B: cyclic lipopeptides identified as the nonribosomal biosynthetic products of Fusarium graminearum

Bahadoor, Adilah; Brauer, Elizabeth K.; Bosnich, Whynn; Schneiderman, Danielle; Johnston, Anne; Aubin, Yves; Blackwell, Barbara; Melanson, Jeremy E.; Harris, Linda J.

Publisher's version / Version de l'éditeur:
https://doi.org/10.1021/jacs.8b10017
Journal of the American Chemical Society, 140, 48, pp. 16783-16791, 2018-11-05

JACS
JOURNAL OF THE AMERICAN CHEMICAL SOCIETY
Article
Cite This: J. Am. Chem. Soc. 2018, 140, 16783−16791
pubs.acs.org/JACS

Gramillin A and B: Cyclic Lipopeptides Identified as the Nonribosomal Biosynthetic Products of *Fusarium graminearum*

Adilah Bahadoor,*,† Elizabeth K. Brauer,‡ Whynn Bosnich,‡ Danielle Schneiderman,‡ Anne Johnston,‡ Yves Aubin,§ Barbara Blackwell,‡ Jeremy E. Melanson,† and Linda J. Harris*,‡

†Metrology, National Research Council Canada, Ottawa, Ontario K1A 0R6, Canada
‡Ottawa Research and Development Centre, Agriculture and Agri-Food Canada, Ottawa, Ontario K1A 0C6, Canada
§Centre for Biologics Evaluation, Biologics, and Genetic Therapies Directorate, Health Canada, Ottawa, Ontario K1A 0K9, Canada

Supporting Information

ABSTRACT: The virulence and broad host range of *Fusarium graminearum* is associated with its ability to secrete an arsenal of phytotoxic secondary metabolites, including the regulated mycotoxins belonging to the deoxynivalenol family. The *TRI* genes responsible for the biosynthesis of deoxynivalenol and related compounds are usually expressed during fungal infection. However, the *F. graminearum* genome harbors an array of unexplored biosynthetic gene clusters that are also co-induced with the *TRI* genes, including the nonribosomal peptide synthetase 8 (*NRPS8*) gene cluster. Here, we identify two bicyclic lipopeptides, gramillin A (**1**) and B (**2**), as the biosynthetic end products of *NRPS8*. Structural elucidation by high-resolution LC-MS and NMR, including ^{1}H-^{15}N-^{13}C HNCO and HNCA on isotopically enriched compounds, revealed that the gramillins possess a fused bicyclic structure with ring closure of the main peptide macrocycle occurring via an anhydride bond. Through targeted gene disruption, we characterized the *GRA1* biosynthetic gene and its transcription factor *GRA2* in the *NRPS8* gene cluster. Further, we show that the gramillins are produced *in planta* on maize silks, promoting fungal virulence on maize but have no discernible effect on wheat head infection. Leaf infiltration of the gramillins induces cell death in maize, but not in wheat. Our results show that *F. graminearum* deploys the gramillins as a virulence agent in maize, but not in wheat, thus displaying host-specific adaptation.

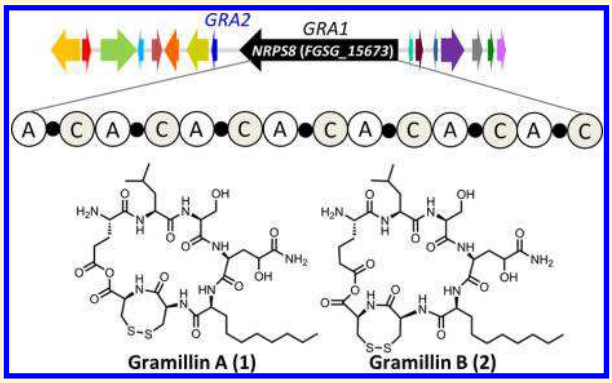

INTRODUCTION

Millions of years of co-evolution have shaped the diverse strategies that fungi use to overcome plant host defenses and establish infection. Perturbation of host defense is often associated with interference with pathogen recognition, suppression of the immune response, disruption of the plant cell structure or metabolism through deployment of proteins, secondary metabolites, or other small molecules.[1] Fungal secondary metabolites are often biosynthesized by enzymes encoded in gene clusters transcribed under specific environmental or developmental conditions,[2] and the hemibiotrophic or necrotrophic fungi are particularly noted for producing toxins that promote plant cell death, disabling immunity and providing the fungus with nutrients.[3]

Fusarium graminearum is a hemibiotrophic pathogen that infects a wide range of plant species including cereal crops such as wheat, maize, and barley.[4] The fungus is a rich source of secondary metabolites, including sesquiterpenoids, polyketides, and nonribosomal peptides. Comparative genomic studies have identified an array of biosynthetic genes encoding terpenoid synthases (TPS), polyketide synthases (PKS), and nonribosomal peptide synthases (NRPS) which are often within co-regulated clusters of genes in the *F. graminearum* genome.[5−7]

Delving into the interactions of *F. graminearum* with maize, barley, and wheat, we revealed that several genes from the *NRPS8* biosynthetic cluster are expressed during infection of maize kernels but exhibited transient expression during barley and wheat spike infection.[8] Furthermore, *NRPS8* was co-expressed alongside the *TRI* biosynthetic genes.[8−10] The *TRI* genes participate in the biosynthesis of the regulated mycotoxin 4-deoxynivalenol, and their involvement in virulence within plant reproductive tissue is well documented.[11−13]

To understand the role of the *NRPS8* gene cluster in infection, we characterized the *GRA1* biosynthetic gene and its transcription factor *GRA2*. We identified the biosynthetic products of *GRA1* as bicyclic lipopeptides, which we named gramillin A and B. Full structure elucidation revealed

Received: September 14, 2018
Published: November 5, 2018

DOI: 10.1021/jacs.8b10017
J. Am. Chem. Soc. 2018, 140, 16783−16791

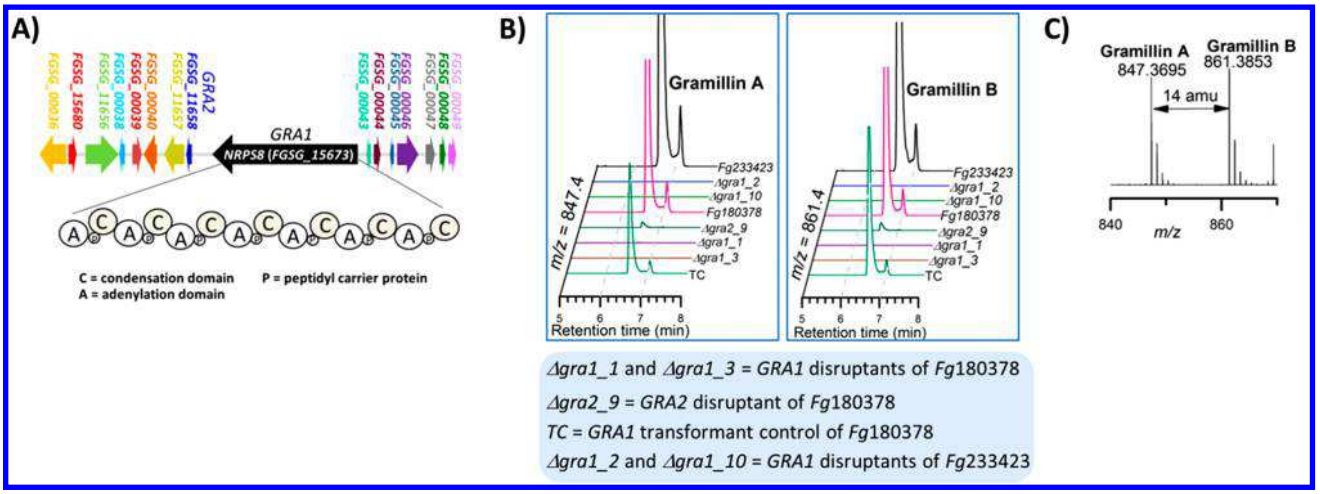

Figure 1. Characterization of *GRA1* and *GRA2* in the *NRPS8* gene cluster. (A) The predicted genes in the *NRPS8* gene cluster include *GRA1* and its transcription factor *GRA2*. *GRA1* encodes the seven-modular NRPS8. (B) Gramillin A and gramillin B co-elute and their production followed by LC-MS from wildtype *Fg*180378 and *Fg*233423 and their respective *GRA1*, *GRA2*, and TC disruptants. (C) The mass spectrum of gramillin A and B.

nonproteinogenic amino acid building blocks, amino acid modifications, and two macrocyclizations that could not be anticipated through sequence analysis.[14,15] Further, *GRA1* is required for full virulence on maize silks, and gramillin A and B induce cell death in maize leaves. During wheat spike infection, the absence of *GRA1* has no effect on virulence, and gramillin A and B do not induce cell death in wheat leaves. Together, this suggests that the gramillins are nonribosomal peptide (NRP) phytotoxins that promote virulence of the pathogen in specific host microenvironments.

■ RESULTS

Gramillin A and B Identified as the Biosynthetic Products of NRPS8. The *NRPS8* gene cluster (*FGSG_00036*−*FGSG_00049*) containing *GRA1* includes the transcription factor *GRA2* and multiple putative peptide tailoring genes (Figure 1A).[5,9] *GRA1* encodes the predicted multimodular 865 kDa NRPS8 containing seven sets of adenylation (A) and condensation (C) domains and peptidyl carrier proteins, indicating the potential incorporation of seven amino acids in the gramillins.[16] *GRA1* was disrupted in the *Fg*180378 and *Fg*233423 wild-type backgrounds via *Agrobacterium*-mediated transformation (Figure S1).[17] A similar strategy was used to disrupt *GRA2* (data not shown). A number of true disruptants were produced as referred to in Figure 1B (see also Table S1). The gene expression of *GRA1* was confirmed to be undetectable or severely reduced in Δ*gra1* and Δ*gra2* mutants by quantitative droplet digital PCR (ddPCR) (Table S2). The secondary metabolite profile of wild-type and Δ*gra1* mutants were compared (Figure 1B and Figures S2−S5). The LC-MS screen revealed a major peak at 6.6 min belonging to a co-eluting mixture of gramillin A (m/z_{obs} = 847.4, $[M + H]^+$) and gramillin B (m/z_{obs} = 861.4, $[M + H]^+$) (Figure 1B,C). Gramillin A, with a molecular formula of $C_{35}H_{58}O_{12}S_2N_8$, was detected as the $[M + H]^+$ ion at an m/z of 847.3695 (m_{calc} 847.3688, $\Delta m = -1.7$ ppm). Similarly, the $[M + H]^+$ ion of gramillin B was detected at an m/z of 861.3853 (m_{calc} 847.3845, $\Delta m = -0.9$ ppm), corresponding to a molecular formula of $C_{36}H_{60}O_{12}S_2N_8$. The mass difference of 14 amu between gramillin A and B already suggested that gramillin B possessed an extra CH_2 group (Figure 1C). A 5-fold reduction in the production of the gramillins was observed from the transformation control strain (TC), and disrupting the transcription factor *GRA2* greatly minimized (>40 fold) the production of the gramillins. Mycelial growth and spore production of the Δ*gra1* (*GRA1* disruption) mutants was similar to wild-type in both genetic backgrounds, while Δ*gra2_9* displayed impaired mycelial growth and conidiation (Supporting Information, Tables S1 and S3). All together, these results point to *GRA1* as a biosynthetic gene leading to the gramillins and *GRA2* as a transcription factor regulating gramillin biosynthesis.

Isolation and Structural Elucidation of Gramillin A and B. To isolate gramillin A and B for structural characterization, a Δ*tri1* mutant of *Fg*180378 was grown in liquid media.[18] Deletion of the *Tri1* gene blocks the final steps in 15-acetyl-4-deoxynivalenol biosynthesis without affecting the production of the gramillins, thereby simplifying their purification from liquid culture (Supporting Information Figure S6). Two major challenges, namely solubility and apparent facile decomposition, stood in the way of isolating and purifying the gramillins from liquid culture. Gramillin A and B are hydrophilic peptides, so biphasic extraction of the aqueous medium with organic solvents was futile. Rather, a solid-phase extraction (SPE) of the aqueous medium provided a crude mixture of gramillin A and B, which after preparative HPLC purification provided a cleaner, but inseparable mixture of the gramillins.

In hindsight, the decomposition of the gramillins was due to the presence of the labile anhydride bond, which we were not aware of at the onset of this study. To circumvent the issue, we speculated that the gramillins must prefer an acidic medium. The pH of the production medium for the gramillins hovers around pH 2−2.5, and no apparent decomposition has been observed under such conditions. Upon switching to acidic phases for isolation and extraction procedures, no decomposition was observed, and enough gramillin material was obtained for NMR. Apart from the complexity of characterizing gramillin A and B as an inseparable mixture, these compounds were also poorly soluble or degraded in a range of solvents. In acidified D_2O, a concentration of up 1 mg/mL of a gramillin A and B mixture was achievable. Alternate NMR

DOI: 10.1021/jacs.8b10017
J. Am. Chem. Soc. 2018, 140, 16783−16791

Scheme 1. Hydrolysis of the Gramillins in Water and Methanol

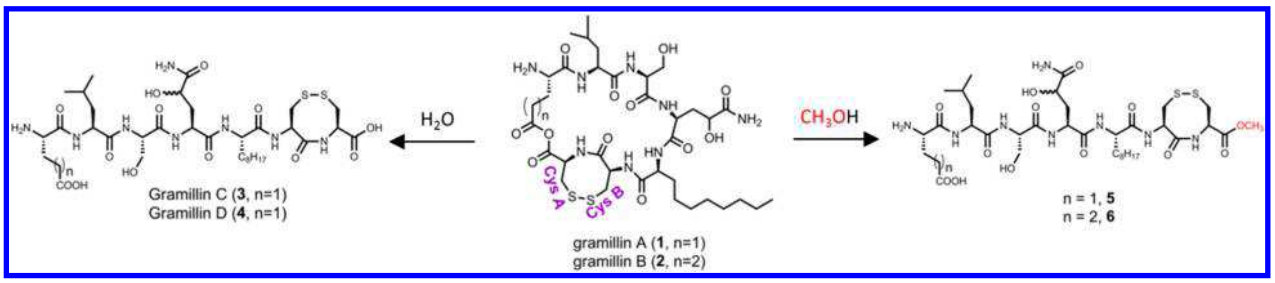

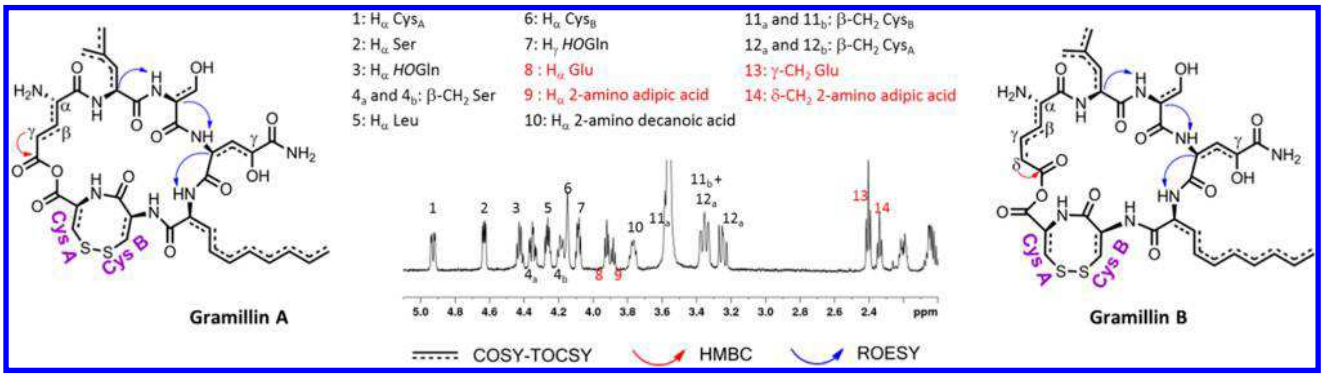

Figure 2. ^{1}H NMR of a gramillin A and B mixture recorded in D_2O:CD_3CN (4:1) + 0.1% formic acid differentiates between the H_α and γ-CH_2 of Glu and the H_α and δ-CH_2 of 2-amino adipic acid. The HMBC recorded in D_2O + 0.1% TFA identifies the carbonyl on the side chains of Glu and 2-amino adipic acid. ROESY correlations determine the partial sequence of Leu-Ser-*HO*Gln-2-amino decanoic acid in the gramillins.

solvents, CD_3OD and DMSO-d_6, were unsuitable due to cross-reactivity with the anhydride bond. Taken together, the pH sensitivity and the cross-reactions with mild nucleophilic solvents, such as methanol and DMSO, pointed toward the presence of a base-sensitive bond in the gramillins.

This inherent sensitivity to mild nucleophiles provided an opportunity to gather crucial structural information about the gramillins. Once enough purified gramillins were obtained, they were exposed to water and methanol, respectively, and their reactions tracked by LC-MS. Upon exposure to water, two new products appeared instantly (Scheme 1). Each contained an extra 18 amu suggesting the incorporation of water. Subsequent MS^2 fragmentations suggested the new products gramillin C (**3**) and gramillin D (**4**) were linear (Figures S7−S8). On the other hand, gramillin A (**1**) and B (**2**) exhibited significantly different MS^2 fragmentation patterns than **3** and **4** (Figures S9−S10). When dissolved in methanol, gramillin A and B hydrolyzed to the new products **5** and **6** with an extra 32 amu, pointing to the incorporation of methanol. MS^2 fragmentation determined that nucleophilic attack by methanol occurred exclusively at the CysA residue with the formation of a methyl ester at the C-terminal Cys A (Figures S11−S12). Both hydrolysis reactions irrevocably rule out a typical macrocylization via an amide bond. Amide bonds are hydrolyzed under harsh acidic or basic conditions. Cyclization via an ester was also ruled out. Methanolysis of ester bonds typically requires an acid catalyst, but the gramillins reacted instantly in water or methanol without any catalyst. Moreover, the molecular formula of the gramillins precluded the presence of an ester bond. On the other hand, an anhydride bond matches the observed molecular formula and is a base-labile bond. Taken together, these observations strongly suggested the existence of an anhydride bond formed from the condensation of the carboxylic acids moieties on the Glu or 2-amino adipic acid side chain to CysA.

Although the presence of serine as one of components of the gramillins was clear by MS^2 fragmentation, the other residues were either unnatural (2-amino decanoic acid and 2-amino adipic acid), modified (*HO*Gln), or isomeric (Leu vs Ile) and thus required NMR for structural confirmation. Furthermore, 1,4-dithiothreitol (DTT) treatment[19] of the gramillins confirmed the presence of a disulfide bond (Figure S13); however, the adjacent position of the two cysteines in the structure was eventually settled by NMR.

Cognizant that the NMR characterization was performed on a gramillin A and B mixture, rather than the individual compounds, it was imperative to obtain NMR spectra with unambiguous signals that would provide clear distinction between gramillin A and B. This was achieved by performing the NMR experiments in different NMR solvent systems, with each providing optimal conditions for observing key correlations to distinguish between gramillin A and B (Figures S14−S17). The ^{1}H-^{1}H COSY and TOCSY coupled to a 1D-proton worked best in D_2O:CD_3CN (4:1) + 0.1% formic acid (Figure 2 and Figures S18−19). From these series of NMR data, the individual amino acid spin systems of two cysteine residues CysA and CysB, Leu, Ser, *HO*Gln and 2-amino decanoic acid were readily established. Furthermore, in the 3−5 ppm region of the spectrum, the α-protons of all the amino acids, as well as the β-CH_2 groups of Ser, CysA, and CysB, appeared as nonoverlapping distinct signals unambiguously confirming their assignments. A clear CH_3-$(CH_2)_n$ COSY-TOCSY correlation indicated the presence of a lipid chain in 2-amino decanoic acid. The α-H signal for the suspected Glu residue did not overlap, producing two visibly separate triplets, thus differentiating gramillin A from gramillin B (Figure 2). The COSY and TOCSY experiments connected the α-CH, β-

DOI: 10.1021/jacs.8b10017
J. Am. Chem. Soc. 2018, 140, 16783−16791

Table 1. ^{1}H and ^{13}C Chemical Shifts of Gramillin A and B in D_2O + 0.1% TFA

Amino Acid	Position	δ_H (*J* in Hz)	δ_C (δ_N)	Amino Acid	Position	δ_H (*J* in Hz)	δ_C (δ_N)
Glutamic acid (gramillin A only)	-NH_2	Not observed		Serine	-NH[a]	8.50 (d, 7.5, gramillin A), 8.47 (d, 7.5, gramillin B)	(115.8)
	α-CH	4.02 (t, 6.6)	52.0		α-CH	4.7 (estimate)	51.1
	β-CH_2	2.10 (m)	25.9		β-CH_2	4.41 (Ha, m), 4.32 (Hb, m)	64.6
	γ-CH_2	2.46 (m)	29.1				
	C=O		168.8				
	C=O (tail)		175.9		C=O		173.7
2-amino-adipic acid (gramillin B only)	-NH_2	Not observed		*HO*-Glutamine	-NH[a]	8.39 (m)	(121.8)
	α-CH	3.96 (t, 6.2)	52.6		α-CH	4.44 (m)	51.8
	β-CH_2	1.84 (m)	30.3		β-CH_2	2.22 (Ha, m),	35.3
	γ-CH_2	1.55 (m)	19.6		γ-CH	2.01 (Hb, m)	68.5
	δ-CH_2	2.38 (t, 7.3)	33.0		C=O	4.14 (dd, 4.5, 8.3)	169.5
	C=O		169.4		$CONH_2$[a]	7.68 (Ha, s),	178.4
	C=O (tail)		177.4			7.17 (Hb, s)	(107.1)
Leucine	-NH[a]	8.66 (d, 6.5, gramillin A), 8.63 (d, 6.5, gramillin B)	(125.2)	2-amino-decanoic acid	-NH[a]	8.79 (m)	(122.0)
	α-CH	4.32 (m)	52.7		α-CH	3.82 (m)	55.7
	β-CH_2	1.55 (m)	39.6		β-CH_2	1.93 (Ha, m), 1.77 (Hb, m)	28.0
	γ-CH	1.55 (m)	24.4		γ-CH_2	1.28 (m)	25.4
	δ(CH_3)	0.86 (d, 5.8), 0.82 (d, 5.4)	22.0 21.1		$(CH_2)_n$ (n=5)	1.18 (m)	22.1, 28.3, 31.2
	C=O		169.3				
					CH_3	0.77 (t, 6.8)	13.6
					C=O		173.1
Cysteine A	-NH[a]	7.63 (d, 11.2)	(114.2)	Cysteine B	-NH[a]	7.82 (s)	(116.3)
	α-CH	5.00 (dt, 3.0, 5.8, 11.4)	55.3		α-CH	4.19 (t, 2.8)	53.9
	β-CH_2	3.37 (Ha, m), 3.3 (Hb, dd, 11.4, 15.2)	46.5		β-CH_2	3.60 (Ha, dd, 2.8. 15.2), 3.43 (Hb, m)	47.1
	C=O		177.4		C=O		174.1

[a] δ_N (shown in parentheses) and δ_H of the NH groups were obtained in H_2O:D_2O (95:5) + 0.1% TFA; δ_N was obtained from the ^{15}N-HSQC spectrum of ^{15}N-enriched gramillin A.

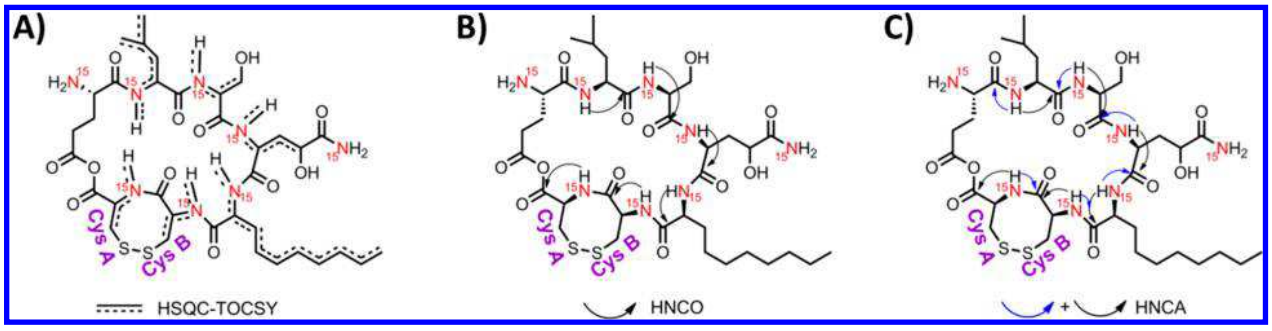

Figure 3. Key ^{1}H-^{15}N-^{13}C NMR correlations. (A) ^{1}H-^{15}N HSQC-TOCSY links the individual amino acid spin system of Leu, Ser, *HO*Gln, 2-amino decanoic acid, Cys B, and Cys A to their respective ^{15}NH. (B) ^{1}H-^{15}N-^{13}C HNCO identifies the amide carbonyls of all the amino acids, except for Glu. (C) ^{1}H-^{15}N-^{13}C HNCA detects the amide carbonyl of Glu and confirms the amino acid sequence of the gramillins.

CH_2, and γ-CH_2 hydrogens of Glu in a three spin system for gramillin A at 4.01, 2.10, and 2.46 ppm, respectively. On the other hand, the TOCSY revealed that the α-CH at 3.96 ppm in gramillin B belonged to a four spin system including three methylene units, whose multiplicities were clearly identified by a phase-sensitive HSQC, at 1.85 (β-CH_2), 1.5−1.6 (γ-CH_2), and 2.38 (δ-CH_2) ppm, respectively.

In D_2O + 0.1% TFA and H_2O:D_2O (95:5) + 0.1% TFA, suppression of the residual water peak eliminated the α-H signal of Ser. On the other hand, ^{1}H-^{13}C HSQC provided reliable proton-carbon correlations. The ^{13}C chemical shifts for all primary, secondary, and tertiary carbon atoms in the gramillins were approximated from the best estimate of the center of the cross-peaks from the HSQC spectrum (Table 1 and Figure S20). All amino acids exhibited similar cross-peaks, except Glu and 2-amino adipic acid. Hydroxylation at the γ-position of *HO*Gln was confirmed by the downfield chemical shift of the γ-H at 4.13 ppm and γ-C at 68.5 ppm. However, the stereochemistry of the γ-OH remains unknown at this point. Two-bond correlations from the HMBC spectrum were used to assign the ^{13}C chemical shifts for the carbonyls in the side-chains of Glu (γ-CH_2 to C=O) and 2-amino adipic acid (δ-CH_2 to C=O) (Figure 2 and Figure S21). The ^{13}C chemical shifts of the amide carbonyls were obtained from ^{15}N NMR. Partial connectivity obtained from a continuous series of ROESY correlations revealed Leu-Ser-*HO*Gln-2-amino decanoic acid was connected in sequence (Figure 2 and Figure S22).

Full connectivity was revealed by ^{15}N NMR experiments, namely ^{15}N-HSQC, HSQC-TOCSY, HNCO, and HNCA

DOI: 10.1021/jacs.8b10017
J. Am. Chem. Soc. 2018, 140, 16783−16791

performed on a ^{15}N-labeled gramillin A and B mixture (gramillin A: gramillin B, ≥ 90:10) (Figures S23−S26). The NH signals of Glu and 2-amino adipic acid were unexpectedly missing from all NMR spectra, in spite of the fact that LC-MS showed all eight nitrogen positions to be enriched (approximately 80% ^{15}N enrichment, Figure S27). The protons of free NH_2 groups have been postulated to undergo fast exchange with water resulting in a reduced signal, which could explain the missing NH signals for Glu and 2-amino adipic acid if their NH_2 groups were free.[20] This observation corroborated MS^2 data on compounds **3** to **6** that also pointed to a free NH_2 group at the Glu and 2-amino adipic acid positions (Figures S7−S8 and S11−S12). The ^{15}N-HSQC and HSQC-TOCSY experiments readily identified the ^{15}NH protons of Leu, Ser, *HO*Gln, 2-amino decanoic acid, Cys A, and Cys B in gramillin A (Figure 3A). In turn, these were linked to their respective carbonyls from the HNCO spectrum (Figure 3B). The HNCA experiment, together with the HNCO data, correlated the inter-residue sequence in gramillin A as Glu-Leu-Ser-*HO*Gln-2-amino decanoic acid-CysB-CysA (Figure 3C). No correlation between the N-terminal of Glu to the C-terminal of CysA was detected in the HNCA spectrum, further confirming that these two residues were not linked via an amide bond and bolstering the hypothesis that the terminal NH_2 group of Glu was free. Rather, it was the HNCA correlation of the ^{15}NH of Leu to the amide carbonyl of Glu that identified its presence, and hence its chemical shift. Altogether, the LC-MS and NMR data indicated the participation of the carboxylic acid group of the Glu and 2-amino adipic acid side chains in the cyclization of the macrocycle via an anhydride bond. To our knowledge, this is the first time an anhydride bond has been implicated in the cyclization of a cyclic peptide.

The absolute stereochemistry of the gramillins was confirmed by chiral LC-MS, after acid hydrolysis. The gramillins hydrolyzed to reveal the L-configurations of Glu (gramillin A only), 2-amino adipic acid (gramillin B only), Leu, Ser, and 2-amino decanoic acid (Figure S28). With NaN_3 in the hydrolysis mixture, the cysteine residues were detected as L-cysteic acid. The absolute stereochemistry of the *HO*Gln residue could not be confirmed by acid hydrolysis. The deamidation of Gln to Glu under acid hydrolysis is documented.[21] A signal potentially belonging to *HO*Glu (m/z_{obs} 164.05516, Δm = −1.2 ppm) was detected from the hydrolysate (Figure S29). However, without an appropriate standard for comparison, its absolute configuration cannot be verified. Alternatively, since no epimerization domains were identified in NRPS8 (Figure 1A), it is likely that *HO*Gln exists in the L-configuration.

The Dynamics of *GRA1* and *TRI1* Co-Expression. With previous research suggesting that the *NRPS8* gene cluster and *TRI* genes are induced under similar conditions,[8−10] we investigated the dynamics and range of gramillin production alongside 15-acetyl-4-deoxynivalenol, the TRI end-product. We monitored *GRA1* (encoding NRPS8, the main biosynthetic gene of the gramillins) gene expression by quantitative ddPCR and gramillin accumulation in the liquid cultures of *Fg*180378, grown in two stages.[22] The first stage medium contains all the requirements for the fungus to undergo exponential growth. After 48 h, the fungus approaches stationary phase. Under these conditions, transient expression of the *GRA1* gene, concomitant with low level detection of the gramillins, is observed. At this point, the rich medium is discarded along with any metabolites produced by the fungus and replaced with a minimal medium for the second stage which induces secondary metabolism (day 0 in Figure 4A). Accordingly,

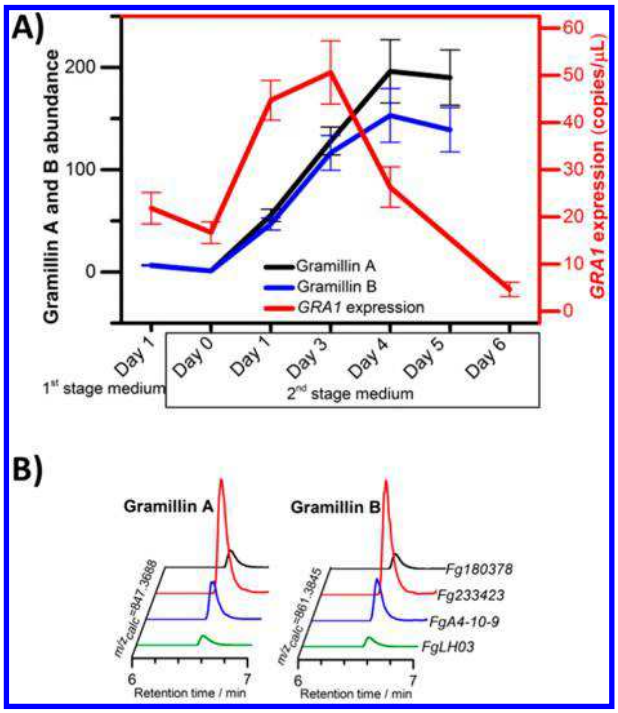

Figure 4. Dynamics and range of gramillin production among *F. graminearum* isolates. (A) Gramillin A and B production, measured relative to Day 0 in 2nd stage medium, closely tracks *GRA1* gene expression. (B) Gramillin A and gramillin B are produced from various *F. graminearum* strains.

GRA1 gene expression rose sharply at day 1 in second stage medium and reached maximum expression levels at day 3, and peak concentrations of gramillin A and B were detected at day 4 (Figure 4A). Expression of the *TRI1* gene and the production of the trichothecene, 15-acetyl-4-deoxynivalenol, also followed the same trend (Figure S30). More importantly, gramillin production did not appear to be influenced by *F. graminearum* chemotype, as a 3-acetyl-4-deoxynivalenol producer (*Fg*LH03) and NX-2 producer (*Fg*A4-10-9) readily produced gramillin A and B (Figure 4B and Figure S31). In addition, Δ*gra1* and Δ*gra2* mutations did not perturb 15-acetyl-4-deoxynivalenol biosynthesis, and a Δ*tri1* mutation had no impact on gramillin production (Figures S6 and S32−S33). These combined observations suggest that while *GRA1* and *TRI* genes are co-expressed, they are involved in distinct biosynthetic processes, thus providing *F. graminearum* the flexibility to exploit either independently or simultaneously depending on its needs.

Gramillins as Host-Specific Virulence Factors. Several genes, including *GRA1*, from the *NRPS8* gene cluster are expressed throughout maize kernel infection and at the beginning of wheat spike infection.[8] To determine if the gramillins modulate plant cell function, a purified inseparable mixture of gramillin A and B was infiltrated into maize and wheat leaves. After 24 h exposure, complete tissue collapse and cell death were observed in maize leaves with 10 μM of gramillin, while wheat leaves remained unaffected (Figure 5A and Figure S34). The effect was dose dependent in maize, where between 1 and 10 μM produced significant cell death and ion leakage within 4 h (Figure 5A,B and Figure S34). To

DOI: 10.1021/jacs.8b10017
J. Am. Chem. Soc. 2018, 140, 16783−16791

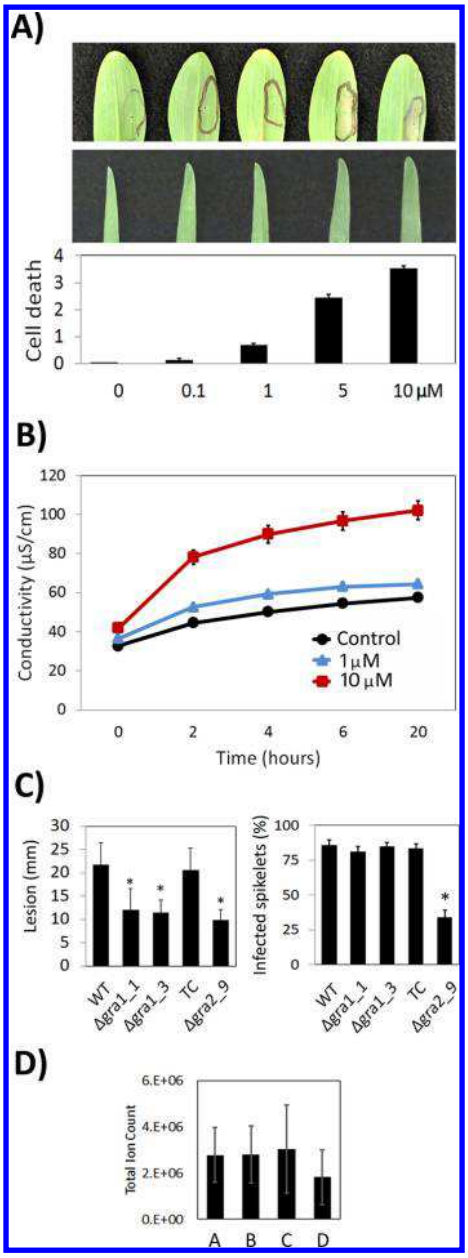

Figure 5. Gramillins are host-specific toxins and virulence factors. (A) Leaves of young maize and wheat plants were infiltrated with the indicated concentrations of the gramillins. Cell death within the infiltrated area was recorded after 24 h by visual assessment (0 indicated no necrosis, 1 = 1−25% necrosis, 2 = 26−50%, 3 = 51−75% and 4 = 76−100% necrosis within the infiltration zone) (n = 20) (Figure S34). (B) Electrolyte leakage in maize leaves (n = 20) measured after exposure to the gramillins or the control. (C) Maize silks and wheat spikelets were inoculated with *Fg*180378, Δ*gra1*, Δ*gra2* disruptants, and transformant control (TC), and extent of disease quantified after 5 days (maize silks, left as lesion size in mm) and 14 days (wheat spikelets, right as % infected spikelets). (D) The gramillins are detected *in planta* on maize silks infected with *Fg*180378 (n = 5). A, gramillin A; B, gramillin B; C, gramillin C; D, gramillin D.

determine if *GRA1* contributes to virulence, wild-type *Fg*180378, Δ*gra1_1*, Δ*gra1_3*, Δ*gra2_9*, and TC conidia were used to inoculate wheat spikes and maize silks (Figure 5C). In maize, both Δ*gra1* and Δ*gra2* strains produced smaller lesions relative to the wild-type and TC strains. Reduced virulence was unrelated to infection structure formation as the mutants were able to form intracellular hyphae and infection cushions similar to the wild-type mutants (Figure S35). In wheat, no differences in infection rate were observed between strains, except for the Δ*gra2_9* mutant. We also analyzed for gramillins in maize silks 5 days after inoculation with *Fg*180378 or Δ*gra1_1* or silks left untreated for the same period. Gramillins (approximately 1:1 cyclic:linear) were only detected in the wild-type *Fg*180378-inoculated silks, but not Δ*gra1_1*-infected or untreated silks (Figure 5D). Together, this indicates that the gramillins are phytotoxins and virulence factors produced by *F. graminearum* in maize and that these functions are attenuated or ineffective in wheat.

■ DISCUSSION

F. graminearum is a virulent plant pathogen infecting a wide variety of cereal crops, thus endangering food supplies, limiting their marketability, and necessitating expensive monitoring and regulation.[23−25] Its versatile ability to adapt to different plant hosts and variable environmental conditions has been linked to its propensity to secrete a diverse array of enzymes and small metabolites. The bioproducts of the *NRPS8* gene cluster are of interest since this gene cluster is co-expressed alongside the trichothecene genes and up-regulated during infection of cereal crops.[8−10,26,27] Here, we identify gramillin A and B as two host-specific virulence factors and NRPS8/GRA1-dependent metabolic products. GRA1 is a hepta-modular NRPS and is a member of the Euascomycete-only synthetases (EAS), a diverse fungal-specific subfamily of NRPS, rendering their amino acid specificity hard to predict by bioinformatic analysis.[28] Therefore, we relied on NMR and LC-MS to elucidate the full structure of the gramillins. Given the structural characterization presented here, more work is necessary to determine if other genes in the *NRPS8* gene cluster (Table 2) are involved in modification of the final product. However, from the predicted functions of some of these genes, their involvement with the biosynthesis of the gramillins is plausible.

Table 2. *NRPS8* Biosynthetic Gene Cluster[5]

gene	predicted function
FGSG_00036	fatty acid synthase (α subunit)
FGSG_15680	cytochrome P450
FGSG_11656	fatty acid CoA synthase (β subunit)
FGSG_00038	hypothetical protein
FGSG_00039	conserved hypothetical protein
FGSG_00040	conserved hypothetical protein, SET domain
FGSG_11657	conserved hypothetical protein
FGSG_11658 (GRA2)	helix−loop−helix transcription factor
FGSG_15673 (GRA1)	NRPS8
FGSG_00043	thioredoxin reductase
FGSG_00044	α/β-hydrolase family
FGSG_00045	α/β-hydrolase family
FGSG_00046	putative multidrug resistance protein
FGSG_00047	α/β-hydrolase family
FGSG_00048	oxidoreductase
FGSG_00049	branched-chain amino acid aminotransferase

The biosynthesis of 2-amino decanoic acid for incorporation in gramillins could be initiated by a fatty acid synthase, of which the α and β subunits[29] are possibly encoded by *FGSG_00036* and *FGSG_11656*, respectively. *FGSG_15680*,

DOI: 10.1021/jacs.8b10017
J. Am. Chem. Soc. 2018, 140, 16783−16791

encoding a cytochrome P450 enzyme related to hydroxylases, could hydroxylate the fatty acid chain. Subsequent oxidation to the ketone by an oxidoreductase (putatively encoded by *FGSG_00048*) and transamination by an aminotransferase (potentially encoded by *FGSG_00049*) could form 2-amino-decanoic acid. On the other hand, *FGSG_15680* could also be responsible for the HO-modified glutamine at the γ-position. Whether hydroxylation occurs on the fully assembled product or on the Gln residue prior to assembly into the gramillins requires further proof. The thioredoxin gene *FGSG_00043* could also be required for the disulfide-bond formation between CysA and CysB. The specific involvement of the remaining genes in the cluster is more difficult to discern, but could have broader regulatory (*FGSG_00040* and *FGSG_11657*) or enzymatic functions (*FGSG_00044* and *FGSG_00045*) based on sequence comparison to orthologous genes. The final C-domain of GRA1 did not possess the expected sequence of a termination C_T domain, often implicated in macrocyclization and release of a cyclopeptide in fungal NRPs (Figure S36).[30] We postulate that in the case of the gramillins, *FGSG_00047*, a thioesterase-encoding gene, perhaps acting in concert with the terminal C-domain of GRA1, can catalyze the formation of the macrocyclic anhydride and release of the products.

Determination of the amino acid specificity of the A domains of GRA1 by ATP-[^{32}P]PP$_i$ exchange assay was beyond the scope of this study. However, with LC-MS and NMR evidence pointing to two adjacent cysteines in the gramillins, it was possible that a high degree of conservation existed between the 10 key positions of the ribosomal code of two adjacent A-domains.[31] More convincingly, based on the Stachelhaus model,[14] the binding pocket codes DVGFLGSIWK of the A-domain of module 6 and DVGFVGSIWK of the A domain of module 7 differed by only one mutation substituting L for V. It is therefore possible that CysB and CysA are encoded by the A-domains of modules 6 and 7. As such, we cautiously propose the biosynthesis of the gramillins to initiate with Glu or 2-amino adipic acid on module 1. Serial annexation of Leu, Ser, *HO*Gln, 2-amino decanoic acid, Cys B, and Cys A then follows by means of modules 2−7, respectively.

A number of nonribosomal peptides (NRP) promote fungal virulence in plants by acting as either siderophores or toxins.[32] Among the 19 predicted *F. graminearum* NRPSs, only NRPS1, NRPS2, NRPS6, NRPS7, and NRPS14 are associated with known products including malonichrome, ferricrocin and fusarinine, as well as fusaristatin and chrysogine.[16,33−36] In addition, NRPS9 has a role in promoting *F. graminearum* virulence on wheat coleoptiles, however the biosynthetic end product remains unknown.[26] The product of NRPS4 may be involved in modifying host surface hydrophobicity but also remains unknown.[37] The gramillins lack the essential hydroxamate moieties to bind Fe^{2+} ions, suggesting that they do not function as siderophores. Fusaristatin A, a PKS-NRPS7 hybrid, is the only other cyclic lipopeptide identified from *F. graminearum* and is a mild antifungal agent.[38] While it appears that all the necessary enzymes to synthesize 2-amino decanoic acid are putatively present in the *NRPS8* gene cluster, for fusaristatin A, the lipid tail is assembled by a PKS gene cluster, then transferred to NRPS7 to be appended to the growing peptide chain.[38]

A thorough search of the literature did not reveal any cyclic peptides containing anhydride bonds, although we found a number of small molecule natural products with maleic anhydride moieties.[39] The maleic acid anhydride-containing natural products share the same pH dependence toward ring stability with the gramillins. In addition, the maleic anhydride structure and, as a result, biological activity were maintained at low pH.[40,41] Alkaline conditions, on the other hand, promote ring opening, leading to biologically inactive compounds. The biological activity of the linear gramillins is currently under investigation. The gramillins share some structural similarity to the malformins, isolated from *Aspergillus niger*, which are cyclic pentapeptides that also possess two cysteines joined in an amide and disulfide bond but lack the lipid tail.[42] Malformins have been reported to inhibit cell elongation to cause root curvature and growth abnormalities in select plants and possess antibacterial activity.[43−45]

We also investigated the relationship between gramillin and trichothecene biosynthesis. In our experiments, 15-acetyl-4-deoxynivalenol production coincided with gramillin production over time, but was unaffected by *GRA1* or *GRA2* expression (Figures S21−22). This suggests that the *NRPS8* and *TRI* gene clusters may be regulated in a similar manner but that their products are not cross-regulating. Numerous transcriptomic studies have profiled *F. graminearum* gene expression during the first few days after plant inoculation. *In vivo*, the *NRPS8* gene cluster is expressed throughout maize kernel infection, but is only expressed transiently in wheat and barley spikes, while *TRI* genes are expressed in all three hosts.[8] Both the *TRI* and *NRPS8* gene clusters are not induced in wheat coleoptiles, while the *NRPS8* cluster is induced at 18 and 48 h post-inoculation during maize stalk infection, whereas the *TRI* genes are not induced.[26,46] The increased expression of *NRPS8* cluster genes in maize relative to other hosts is interesting when considering that gramillin is a virulence factor and phytotoxin in maize but not in wheat. *GRA1* disruption did not impair growth *in vitro*, as expected for a gene involved in secondary metabolism, but did inhibit maize silk infection. Disruption of *GRA2* appeared to have more pleiotropic effects and probably influences genes outside of the *NRPS8* gene cluster, reflected in reduced growth on solid media and consequently reduced virulence on both maize and wheat.

These observations support the idea that *F. graminearum* responds to host-specific cues to deploy only the virulence factors that are effective within a host microenvironment. However, the mechanisms underlying fungal perception of the host environment remain unknown, and the identity and host specificity of virulence factors remain masked by functional redundancy.[47] In addition, our observation that wheat remains insensitive to gramillin may provide avenues for developing resistance in maize. For example, wheat cells may be detoxifying or sequestering gramillin, or wheat may lack a host susceptibility factor. Manipulation of similar genes and processes in maize could have an impact on pathogen virulence and disease progression. Overall, the discovery of the gramillins as disease-promoting metabolites furthers our understanding of the biosynthetic capabilities and attack strategies of the *F. graminearum* fungal pathogen.

■ ASSOCIATED CONTENT

Supporting Information

The Supporting Information is available free of charge on the ACS Publications website at DOI: 10.1021/jacs.8b10017.

DOI: 10.1021/jacs.8b10017
J. Am. Chem. Soc. 2018, 140, 16783−16791

All supplementary figures (Figures S1 to S36) and tables (Tables S1−S5) mentioned in this report and full experimental details (PDF)

■ AUTHOR INFORMATION

Corresponding Authors

*Adilah.Bahadoor@nrc-cnrc.gc.ca

*Linda.Harris@canada.ca

ORCID

Adilah Bahadoor: 0000-0002-8130-5070

Notes

The authors declare no competing financial interest.

■ ACKNOWLEDGMENTS

We thank Dr. Juris Meija of the National Research Council Canada, developer of the ^{15}N calculator, for assistance in calculating ^{15}N incorporation in the gramillins.

■ REFERENCES

(1) Rodriguez-Moreno, L.; Ebert, M. K.; Bolton, M. D.; Thomma, B. P. Tools of the Crook-Infection Strategies of Fungal Plant Pathogens. *Plant J.* **2018**, *93*, 664−674.

(2) Brakhage, A. A.; Schroeckh, V. Fungal Secondary Metabolites - Strategies to Activate Silent Gene Clusters. *Fungal Genet. Biol.* **2011**, *48*, 15−22.

(3) Scharf, D. H.; Heinekamp, T.; Brakhage, A. A. Human and Plant Fungal Pathogens: The Role of Secondary Metabolites. *PLoS Pathog.* **2014**, *10*, No. e1003859.

(4) Kazan, K.; Gardiner, D. M.; Manners, J. M. On the Trail of a Cereal Killer: Recent Advances in *Fusarium graminearum* Pathogenomics and Host Resistance. *Mol. Plant Pathol.* **2012**, *13*, 399−413.

(5) Sieber, C. M. K.; Lee, W.; Wong, P.; Münsterkötter, M.; Mewes, H.-W.; Schmeitzl, C.; Varga, E.; Berthiller, F.; Adam, G.; Güldener, U. The *Fusarium graminearum* Genome Reveals More Secondary Metabolite Gene Clusters and Hints of Horizontal Gene Transfer. *PLoS One* **2014**, *9*, No. e110311.

(6) Ma, L.-J.; Geiser, D. M.; Proctor, R. H.; Rooney, A. P.; O'Donnell, K.; Trail, F.; Gardiner, D. M.; Manners, J. M.; Kazan, K. *Fusarium* Pathogenomics. *Annu. Rev. Microbiol.* **2013**, *67*, 399−416.

(7) Ma, L.-J; Van der Does, H. C.; Borkovich, K. A.; Coleman, J. J.; Daboussi, M.-J.; Di Pietro, A.; Dufresne, M.; Freitag, M.; Grabherr, M.; Henrissat, B.; Houterman, P. M.; Kang, S.; Shim, W.-B.; Woloshuk, C.; Xie, X.; Xu, J.-R.; Antoniw, J.; Baker, S. E.; Bluhm, B. H.; Breakspear, A.; Brown, D. W.; Butchko, R. A. E.; Chapman, S.; Coulson, R.; Coutinho, P. M.; Danchin, E. G.; Diener, A.; Gale, L. R.; Gardiner, D. M.; Goff, S.; Hammond-Kosack, K. E.; Hilburn, K.; Hua-Van, A.; Jonkers, W.; Kazan, K.; Kodira, C. D.; Koehrsen, M.; Kumar, L.; Lee, Y.-H.; Li, L.; Manners, J. M.; Miranda-Saavedra, D.; Mukherjee, M.; Park, G.; Park, J.; Park, S.-Y.; Proctor, R. H.; Regev, A.; Ruiz-Roldan, M. C.; Sain, D.; Sakthikumar, S.; Sykes, S.; Schwartz, D. C.; Turgeon, B. G.; Wapinski, I.; Yoder, O.; Young, S.; Zeng, Q.; Zhou, S.; Galagan, J.; Cuomo, C. A.; Kistler, H. C.; Rep, M. Comparative Genomics Reveals Mobile Pathogenicity Chromosomes in *Fusarium*. *Nature* **2010**, *464*, 367−373.

(8) Harris, L. J.; Balcerzak, M.; Johnston, A.; Schneiderman, D.; Ouellet, T. Host-preferential *Fusarium graminearum* Gene Expression During Infection of Wheat, Barley, and Maize. *Fungal Biol.* **2016**, *120*, 111−123.

(9) Gardiner, D. M.; Kazan, K.; Manners, J. M. Novel Genes of *Fusarium graminearum* That Negatively Regulate Deoxynivalenol Production and Virulence. *Mol. Plant-Microbe Interact.* **2009**, *22*, 1588−1600.

(10) Jonkers, W.; Dong, Y.; Broz, K.; Kistler, H. C. The Wor1-like Protein Fgp1 Regulates Pathogenicity, Toxin Synthesis and Reproduction in the Phytopathogenic Fungus *Fusarium graminearum*. *PLoS Pathog.* **2012**, *8*, No. e1002724.

(11) Proctor, R. H.; Hohn, T. M.; McCormick, S. P. Reduced Virulence of Gibberella zeae Caused by Disruption of a Trichothecene Toxin Biosynthetic Gene. *Mol. Plant-Microbe Interact.* **1995**, *8*, 593−601.

(12) Harris, L. J.; Desjardins, A. E.; Plattner, R. D.; Nicholson, P.; Butler, G.; Young, J. C.; Weston, G.; Proctor, R. H.; Hohn, T. M. Possible Role of Trichothecene Mycotoxins in Virulence of *Fusarium graminearum* on Maize. *Plant Dis.* **1999**, *83*, 954−960.

(13) Langevin, F.; Eudes, F.; Comeau, A. Effect of Trichothecenes Produced by *Fusarium graminearum* During *Fusarium* Head Blight Development in Six Cereal Species. *Eur. J. Plant Pathol.* **2004**, *110*, 735−746.

(14) Stachelhaus, T.; Mootz, H. D.; Marahiel, M. A. The Specificity-Conferring Code of Adenylation Domains in Nonribosomal Peptide Synthases. *Chem. Biol.* **1999**, *6*, 493−505.

(15) Challis, G. L.; Ravel, J.; Townsend, C. A. Predictive, Structure-Based Model of Amino Acid Recognition by Nonribosomal Peptide Synthetase Adenylation Domains. *Chem. Biol.* **2000**, *7*, 211−224.

(16) Hansen, F. T.; Gardiner, D. M.; Lysøe, E.; Fuertes, P. R.; Tudzynski, B.; Wiemann, P.; Sondergaard, T. E.; Giese, H.; Brodersen, D. E.; Sørensen, J. L. An Update to Polyketide Synthase and Non-Ribosomal Synthetase genes and Nomenclature in *Fusarium*. *Fungal Genet. Biol.* **2015**, *75*, 20−29.

(17) Frandsen, R. J. N.; Frandsen, M.; Giese, H. In *Plant Fungal Pathogens: Methods and Protocols*; Bolton, D., Thomma, B. P. H. J., Eds.; Springer Science+Business Media: New York, 2012; Vol. *835*, p 17−45.

(18) McCormick, S. P.; Harris, L. J.; Alexander, N. J.; Ouellet, T.; Saparno, A.; Allard, S.; Desjardins, A. E. Tri1 in *Fusarium graminearum* Encodes a P450 Oxygenase. *Appl. Environ. Microbiol.* **2004**, *70*, 2044−2051.

(19) Scigelova, M.; Green, P. S.; Giannakopulos, A. E.; Rodger, A.; Crout, D. H. G.; Derrick, P. J. A Practical Protocol for the Reduction of Disulfide Bonds in Proteins Prior to Analysis by Mass Spectrometry. *Eur. J. Mass Spectrom.* **2001**, *7*, 29−34.

(20) Schmidt, J. M.; Thuring, H.; Werner, A.; Ruterjans, H.; Quaas, R.; Hahn, U. Two-dimensional ^{1}H, ^{15}N-NMR Investigation of Uniformly ^{15}N-labeled Ribonuclease T1. *Eur. J. Biochem.* **1991**, *197*, 643−653.

(21) Li, X.; Lin, C.; O'Connor, P. B. Glutamine Deamidation: Differentiation of Glutamic Acid and gamma-Glutamic Acid in Peptides by Electron Capture Dissociation. *Anal. Chem.* **2010**, *82*, 3606−3615.

(22) Miller, J. D.; Blackwell, B. A. Biosynthesis of 3-acetyldeoxynivalenol and Other Metabolites by *Fusarium culmorum* HLX 1503 in a Stirred Jar Fermentor. *Can. J. Bot.* **1986**, *64*, 1−5.

(23) Marin, S.; Ramos, A.; Cano-Sancho, G.; Sanchis, V. Mycotoxins: Occurrence, Toxicology, and Exposure Assessment. *Food Chem. Toxicol.* **2013**, *60*, 218−237.

(24) Wilson, W.; Dahl, B.; Nganje, W. Economic Costs of *Fusarium* Head Blight, Scab and Deoxynivalenol. *World Mycotoxin J.* **2018**, *11*, 291−302.

(25) Ferrigo, D.; Raiola, A.; Causin, R. *Fusarium* Toxins in Cereals: Occurrence, Legislation, Factors Promoting the Appearance and Their Management. *Molecules* **2016**, *21*, 627.

(26) Zhang, X.; Jia, L.; Zhang, Y.; Jiang, G.; Li, X.; Zhang, D.; Tang, W. *In planta* Stage-Specific Fungal Gene Profiling Elucidates the Molecular Strategies of *Fusarium graminearum* Growing Inside Wheat Coleoptiles. *Plant Cell* **2012**, *24*, 5159−5176.

(27) Stephens, A. E.; Gardiner, D. M.; White, R. G.; Munn, A. L.; Manners, J. M. Phases of Infection and Gene Expression of *Fusarium graminearum* During Crown Rot Disease of Wheat. *Mol. Plant-Microbe Interact.* **2008**, *21*, 1571−1581.

(28) Bushley, K. E.; Turgeon, B. G. Phylogenomics Reveals Subfamilies of Fungal Nonribosomal Peptide Synthetases and Their Evolutionary Relationships. *BMC Evol. Biol.* **2010**, *10*, 26.

(29) Singh, N.; Wakil, S. J.; Stoops, J. K. Yeast Fatty Acid Synthase: Structure to Function Relationship. *Biochemistry* **1985**, *24*, 6598−6602.

DOI: 10.1021/jacs.8b10017
J. Am. Chem. Soc. 2018, 140, 16783−16791

(30) Gao, X.; Haynes, S. W.; Ames, B. D.; Wang, P.; Vien, L. P.; Walsh, C. T.; Tang, Y. Cyclization of Fungal Nonribosomal Peptides by a Terminal Condensation-like Domain. *Nat. Chem. Biol.* **2012**, *8*, 823−830.
(31) Kalb, D.; Lackner, G.; Hoffmeister, D. Fungal Peptide Synthetases: An Update on Functions and Specificity Signatures. *Fung. Biol. Rev.* **2013**, *27*, 43−50.
(32) Hoffmeister, D.; Keller, N. P. Natural Products of Filamentous Fungi: Enzymes, Genes, and Their Regulation. *Nat. Prod. Rep.* **2007**, *24*, 393−416.
(33) Oide, S.; Berthiller, F.; Wiesenberger, G.; Adam, G.; Turgeon, B. G. Individual and Combined roles of Malonichrome, Ferricrocin, and TAFC Siderophores in *Fusarium graminearum* Pathogenic and Sexual Development. *Front. Microbiol.* **2015**, *5*, 759.
(34) Tobiasen, C.; Aahman, J.; Ravnholt, K. S.; Bjerrum, M. J.; Grell, M. N.; Giese, H. Nonribosomal Peptide Synthetase (NPS) genes in *Fusarium graminearum*, *F. culmorum* and *F. pseudograminearium* and Identification of NPS2 as the Producer of Ferricrocin. *Curr. Genet.* **2007**, *51*, 43−58.
(35) Varga, J.; Kocsube, S.; Toth, B.; Mesterhazy, A. Nonribosomal Peptide Synthetase Genes in the Genome of *Fusarium graminearum*, Causative Agent of Wheat Head Blight. *Acta Biol. Hung.* **2005**, *56*, 375−388.
(36) Wollenberg, R. D.; Saei, W.; Westphal, K. R.; Klitgaard, C. S.; Nielsen, K. L.; Lysøe, E.; Gardiner, D. M.; Wimmer, R.; Sondergaard, T. E.; Sørensen, J. L. Chrysogine Biosynthesis is Mediated by a Two-module Nonribosomal Peptide Synthetase. *J. Nat. Prod.* **2017**, *80*, 2131−2135.
(37) Hansen, F. T.; Droce, A.; Sorensen, J. L.; Fojan, P.; Giese, H.; Sondergaard, T. E. Overexpression of NRPS4 Leads to Increased Surface Hydrophobicity in *Fusarium graminearum*. *Fungal Biol.* **2012**, *116*, 855−862.
(38) Sorensen, J. L.; Sondergaard, T. E.; Covarelli, L.; Fuertes, P. R.; Hansen, F. T.; Frandsen, R. J. N.; Saei, W.; Lukassen, M. B.; Wimmer, R.; Nielsen, K. F.; Gardiner, D. M.; Giese, H. Identification of the Biosynthetic Gene Clusters for the Lipopeptides Fusaristatin A and W493B in *Fusarium graminearum* and *F. pseudograminearum*. *J. Nat. Prod.* **2014**, *77*, 2619−2625.
(39) Chen, X.; Zheng, Y.; Shen, Y. Natural Products with Maleic Anhydride Structure: Nonadrides, Tautomycin, Chaetomellic Anhydride, and Other Compounds. *Chem. Rev.* **2007**, *107*, 1777−1830.
(40) Singh, S. B.; Zink, D. L.; Liesch, J. M.; Goetz, M. A.; Jenkins, R. G.; Nallin-Omstead, M.; Silverman, K. C.; Bills, G. F.; Mosley, R. T.; Gibbs, J. B.; Albers-Schonberg, G.; Lingham, R. B. Isolation and Structure of Chaetomellic Acid A and B from *Chaetomella acutiseta*: Farnesyl Pyrophosphate Mimic Inhibitors of Ras Farnesyl-Protein Transferase. *Tetrahedron* **1993**, *49*, 5917−5926.
(41) Futagawa, M.; Rimando, A. M.; Tellez, M. R.; Wedge, D. E. pH Modulation of Zopfiellin Antifungal Activity to *Colletotrichum* and *Botrytis*. *J. Agric. Food Chem.* **2002**, *50*, 7007−7012.
(42) Cutler, H. G. Microbial Natural Products that Affect Plants, Phytopathogens, and Certain Other Microorganisms. *Crit. Rev. Plant Sci.* **1995**, *14*, 413−444.
(43) Suda, S.; Curtis, R. W. Antibiotic Properties of Malformin. *Appl. Microbiol.* **1966**, *14*, 475−476.
(44) Izhar, S.; Bevington, J. M.; Curtis, R. W. Effect of Malformin on Root Growth. *Plant Cell Phys.* **1969**, *10*, 687−698.
(45) Curtis, R. W. Studies on Response of Bean Seedlings and Corn Roots to Malformin. *Plant Physiol.* **1961**, *36*, 37−43.
(46) Zhang, Y.; He, J.; Jia, L.-J.; Yuan, T.-L.; Zhang, D.; Guo, Y.; Wang, Y.; Tang, W.-H. Cellular Tracking and Gene Profiling of *Fusarium graminearum* During Maize Stalk Rot Disease Development Elucidates Its Strategies in Confronting Phosphorus Limitation in the Host Apoplast. *PLoS Pathog.* **2016**, *12*, No. e1005485.
(47) Adam, G.; Wiesenberger, G.; Güldener, U. In *Biosynthesis and Molecular Genetics of Fungal Secondary Metabolites*; Springer: New York, 2015; Vol. 2, p 199−233.

DOI: 10.1021/jacs.8b10017
J. Am. Chem. Soc. 2018, 140, 16783−16791